Elastic properties of grain boundaries in copper and their relationship to bulk elastic constants

James B. Adams, Wilhelm G. Wolfer, and Stephen M. Foiles
Theoretical Division, Sandia National Laboratories, Livermore, California 94550
(Received 7 June 1989)

The pressure derivatives and uniaxial strain derivatives of the elastic constants of copper are calculated using the embedded-atom method, and the results are in good agreement with experiment. Also, the elastic constants of a $\Sigma 5$ twist grain boundary [with (100) boundary planes] are calculated on a layer-by-layer basis, and the elastic behavior is shown to differ by up to an order of magnitude from bulklike behavior. This unusual elastic behavior is found to be similar to that of uniaxially strained crystals, since the grain boundaries themselves are regions that are strained (expanded) in one direction.

I. INTRODUCTION

The structure and mechanical properties of grain boundaries have been subjects of recent experimental[1-7] and theoretical interest.[7-16] Both transmission electron microscopy (TEM) (Refs. 2 and 3) and x-ray diffraction[4-7] techniques are currently used to pinpoint the location of atoms at grain boundaries. Theoretical calculations by Foiles[12,13] using the embedded-atom method (EAM) (Refs. 17 and 18) are in good agreement with experiment for the $\Sigma 5$ tilt and $\Sigma 13$ twist boundaries in Au. (An unresolved controversy exists for the $\Sigma 5$ twist boundary in Au; two experimental groups using x-ray diffraction have suggested different structures; EAM calculations agree with one of the structures.[7])

The EAM has also been applied by Wolf and coworkers[14,15] to the study of the elastic properties of grain boundaries, both in thin slabs and in superlattices. They found that several typical grain boundaries have a larger (than bulk) Young's modulus (E) in the direction normal to the boundary, and a much weaker shear modulus (G) parallel to the boundary. They found the same qualitative features using pair potentials.[14,15] Phillpot, Lutsko, and Wolf have also studied elastic constants of grain boundaries in silicon.[16]

Wolf and Lutsko[14] carefully compared radial distributions of atoms in the bulk and at grain boundaries. They found that atoms at the grain boundary were generally farther separated from one another, although approximately 10% of the atoms were closer. They also calculated the Young's modulus E and shear modulus G of a perfect crystal as a function of lattice constant, and found that expansions of the lattice tended to decrease both E and G. Since a grain boundary is an expanded region (relative to the bulk), one might expect *both* E and G to decrease, in contrast with their results.

However, since grain boundaries are only expanded in one dimension (perpendicular to the interface), then their elastic properties are expected to be similar to those of crystals expanded in one dimension, not three.

The purpose of this paper is to present an explanation of the elastic behavior of grain boundaries. First, we further establish the reliability of the embedded-atom method by demonstrating that it correctly predicts the pressure and uniaxial-strain derivatives of the elastic constants of copper. These results strongly suggest that the calculated elastic constants of deformed materials, such as grain boundaries, will be similarly realistic. Second, we calculate E and G for a $\Sigma 5$ twist boundary in copper, and suggest a simple relationship between the elastic behavior of twist grain boundaries and uniaxially strained crystals.

It should be pointed out that we have previously established that the EAM accurately predicts both thermal expansion (which is related to the derivatives of the elastic constants)[19,20] and the derivative of the elastic constants with respect to interstitial concentration.[21] These results further suggest that the EAM will reliably model the elastic properties of defected regions such as grain boundaries.

II. EMBEDDED-ATOM METHOD AND ITS APPLICATION

The EAM is a model of metallic cohesion developed by Daw and Baskes.[17] It is a semiempirical model whose functions are developed by fitting to experimental data, such as lattice constant, sublimation energy, elastic constants, and vacancy-formation energy.[18] It is analogous to pair potentials, but it includes many-body terms to properly describe metallic bonding. Summaries of the EAM have been given previously, and we will not reproduce them here. In this work we use the EAM functions for copper from Ref. 18.

The EAM has been shown to accurately predict many physical properties, such as vacancy and interstitial properties,[18] phonon dispersion,[22] liquid metal structure,[23] alloys,[18] bulk diffusion in metals and alloys,[24,25] Gibb's free energies,[20] and the structure of grain boundaries.[7,12,13] It has also been applied to calculating properties of sur-

faces, including surface energies,[18] surface relaxations,[18] surface reconstructions,[26–29] surface segregation,[30,31] and phonon dispersion at surfaces.[32,33] The ability of the EAM to accurately describe such a wide range of properties is one of the most surprising and powerful justifications of the approach.

The EAM calculations described in this work could have been carried out either analytically or computationally. Whereas Wolf and Lutsko used an analytic approach[34] to calculate the elastic properties, we chose the computational approach, because it is simpler to carry out and can be easily applied to defected regions such as grain boundaries. Using our numerical approach, elastic constants could generally be calculated to only four significant figures, due to a small amount of numerical "noise." The cause of the noise is due to the fact that the EAM functions are defined numerically on a grid; they are determined by a four-point Lagrange interpolation between grid points.

The calculation of pressure and strain derivatives of the bulk material involved systems of 256 atoms (288 for calculating C_{44}). Adjustable periodic boundary conditions were applied, using a modification of the algorithm of Parinello and Raman.[35] The calculations were carried out at 0 K, using molecular statics (MS), in which atomic positions are adjusted by a conjugate gradient method so as to minimize the total energy. Calculations at finite temperatures could have been carried out using molecular dynamics; however, such calculations would have been much more computationally expensive. Since the elastic constants at 0 K are generally within 10% of those at room temperature, where the experiments were carried out, our results should be comparable with the experimental values.

Calculations involving the $\Sigma 5$ grain boundary involved an orthorhombic system of 1600 atoms, approximately $14.5\times14.5\times72.3$ Å. The grain boundary was aligned perpendicular to the longest axis, with (100) boundary planes. The surfaces perpendicular to the boundary were treated with periodic boundary conditions, and the two surfaces parallel to the boundary were "free," or solid-vacuum interfaces. Although the use of free surfaces creates inaccuracies in the results near the surface, we demonstrate in Sec. III D that these effects are small and limited to only a few layers near the surface. Periodic boundary conditions could have been used instead of free surfaces, resulting in a periodic arrangement of grain boundaries; however, our results show that the grain boundaries affect the mechanical properties somewhat more than free surfaces. Also, this choice of boundary conditions allows the two crystals to shift relative to one another.

The structure of the boundary was determined by beginning with a coincident-site lattice (CSL) and then performing a simple MS calculation to determine the minimum-energy configuration. The resulting structure was also annealed at 500 K using MC techniques, and after cooling back to 0 K the same crystal structure resulted. These results strongly suggest, although they do not prove, that the final structure was the lowest-energy configuration.

III. RESULTS AND DISCUSSION

A. Pressure derivatives

The hydrostatic pressure derivatives of the elastic constants were calculated by determining the elastic constants at five pressures, from 10 to -10 kbar. The elastic constants were found to vary linearly, so their derivatives could be easily calculated.

For a given pressure, the elastic constants were calculated by slightly varying the pressure in different directions, and determining the corresponding strain of the crystal. The details of this procedure are listed in Table I. For example, the Young's modulus E was calculated by varying the pressure in the x direction, with the y and z dynamic boundaries were allowed to adjust (Poisson contraction allowed).

For C_{44}, we used a crystal which was rotated 45° to the reference lattice, so that its [110] direction was oriented along the x axis. This orientation allowed a simple determination of C_{44} (see Table I).

Table II compares the calculated pressure derivatives with experimental measurement.[36–38] The calculated values for the bulk modulus B and the shear modulus C_{44} are 80–90 % of the experimental values, and the calculated value for the shear modulus $G=(C_{11}-C_{12})/2$ is in the middle of the range of experimental values.

B. Uniaxial strain derivatives of the Young's modulus

Although the uniaxial strain derivatives of the elastic constants have not in general been determined experimentally, the strain derivatives of the Young's modulus have been determined for several materials (see Milstein and Rasky[39]). The total strain ϵ of a crystal subject to a tensile stress σ is usually expressed as

$$\epsilon=\frac{\sigma}{E_0}+\delta\left[\frac{\sigma}{E_0}\right]^2, \tag{1}$$

where E_0 is the Young's modulus at zero strain, and δ is a materials constant. For most fcc metals (including copper), δ is negative in the [100] direction and positive in the [110] and [111] directions.[38] In other words, the effective Young's modulus increases for [100] strains and decreases for [110] and [111] strains.

We used the EAM to calculate δ for copper, using an

TABLE I. Method for calculation of the elastic constants. σ is the pressure applied in a given direction. The asterisk indicates that the crystal is rotated 45° relative to the reference lattice.

Elastic constant	Pressure x	y	z
G	σ	$-\sigma$	
C_{44}	σ^*	$-\sigma^*$	
B	σ	σ	σ
E	σ		

TABLE II. Pressure derivatives of the elastic constants of copper.

Method	B	C_{44}	G
EAM	4.5	2.1	0.47
Expt. (Ref. 36)	5.59	2.35	0.580
Expt. (Ref. 37)	5.44	2.63	0.375
Expt. (Ref. 38)	5.32	2.36	0.45

approach similar to that for pressure derivatives. In other words, the Young's modulus was calculated by applying uniaxial stresses and determining the resulting strain; *the Poisson contraction was allowed* by using dynamic boundary conditions. Allowing for the Poisson contaction is, of course, necessary to accurately calculate the Young's modulus. δ was found to have a small strain dependence, so we averaged the values over small strains corresponding to typical experimental ranges, namely 1% strains for the [100] and [111] directions and 2% strains for the [110] direction. Although these strains are large enough to plastically deform polycrystalline materials, the experiments on single crystals[40,41] determined that the measured strains were elastic (no hysteresis in the stress-strain curves).

Table III presents the EAM calculations of δ and compares them with both experiment[40,41] and the theoretical calculations by Milstein and Rasky[39] using Morse potentials. Both theory and experiment are in excellent qualitative agreement. The quantitative agreement is also excellent for the [100] [110] directions; in the [111] direction the experimental values range from 2.1 to 3.76, whereas both theories yield low values (1.6–1.7), suggesting that the actual experimental value is in the lower range of the experimental results.

Table III also lists the Young's moduli for the different directions. The Morse potential is fit to the Young's modulus in the [100] direction, but cannot exactly fit the Young's moduli in the [110] and [111] directions since C_{12} must equal C_{44} for a pair potential. Since the EAM contains a many-body term, it can accurately fit the Young's moduli in all directions. The Morse model was fit to elastic constants at 0 K, whereas the EAM was fit to elastic constants at 300 K. It is interesting to note that although both models yielded good agreement with the experimental results for δ (see Table III), the EAM's absolute value of the Young's modulus is more reliable in the [110] and especially the [111] directions.

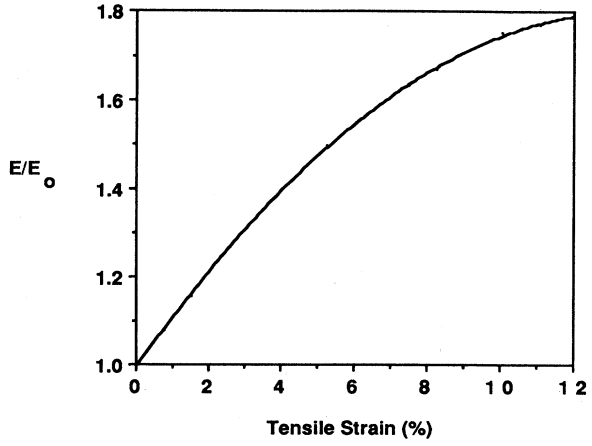

FIG. 1. The effective Young's modulus (for infinitesimal strains) in the [100] direction as a function of strain in the [100] direction.

Figure 1 graphs the effective Young's modulus in the [100] direction for infinitesimal strain as a function of total strain in the [100] direction. For large strains, the Young's modulus is found to vary nonlinearly as a function of strain.

C. Strain derivatives of the shear modulus

The EAM was also used to calculate the uniaxial strain derivative of the shear modulus C_{44} for shear perpendicular to the uniaxial strain. In order to compare the results more directly with those for grain boundaries (see Sec. III D), the crystal was strained in one direction *without allowing for a Poisson contraction.* Although we could have allowed for a Poisson contraction, we wished to compare our results with the structure of grain boundaries, which are approximately regions strained in 1 dimension without a Poisson contraction. Allowing for a Poisson contraction only slightly changes the shear modulus (about a 7% change at an 8% uniaxial strain).

TABLE III. Young's moduli and nonlinearity constant δ for copper. The EAM calculations were carried out at 0 K, but were fit to elastic-constant data at room temperature. The Morse potentials were carried out at 0 K, and were fit to 0 K elastic constants. The asterisk denotes experimental values at 300 K. The double asterisk denotes values at 0 K.

Method	E_{100}	E_{110}	E_{111}	δ_{100}	δ_{110}	δ_{111}
EAM	0.616	1.256	1.939	−4.3±0.2	10.5±0.5	1.6±0.2
Expt. (Ref. 39)*	0.667	1.303	1.911			
Expt. (Ref. 40)				−4.3±0.5	10.0±0.5	3.5±0.1
Expt.[a]				−4.51	10.57	3.76
Expt. (Ref. 41)				−4.4±0.2	8.9±0.7	2.1±0.7
Expt. (Ref. 39)**	0.726	1.411	2.059			
Morse (Ref. 39)	0.726	1.658	2.897	−6.0	10.0	1.7

[a]Calculated (Ref. 40) from experimental data (Ref. 37).

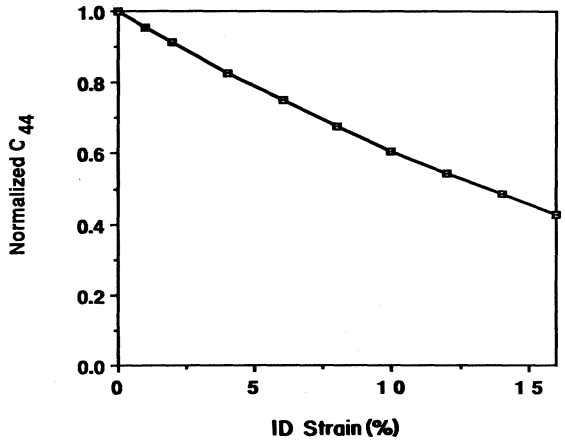

FIG. 2. The shear modulus C_{44} (for infinitesimal shears) as a function of strain (without Poisson contraction) in the [100] direction.

The shear modulus was then calculated by applying a shear strain to the crystal and calculating the second derivative of the crystal's enthalpy. Figure 2 plots C_{44} as a function of uniaxial strain.

D. Elastic behavior of a Σ5 twist grain boundary

As discussed in Sec. II, the structure of the grain boundary is fairly similar to that of the CSL lattice. Figure 3 plots the average interplanar spacing between the planes parallel to the boundary; even at the grain boundary the atoms remain within 0.2 Å of the average. The plot clearly demonstrates that there is a large expansion in the interplanar spacing at the boundary, but that the other planes are not significantly affected. The change in lattice spacing at the surface is seen to be relatively small and not to extend more than a few layers into the material.

Also, it should be noted that in the bulklike region between the grain boundary and the free surface, the interatomic spacing is 1.822 Å instead of 1.807 Å. This change is due to a contraction of the slab in the direction parallel to the boundary, in order to minimize the surface area; the contraction results in a Poisson expansion of the slab perpendicular to the boundary. This change in the lattice spacing is purely a result of the finite size of the slab; for larger slabs, the effect is smaller. This small change in the lattice spacing has a small effect on the elastic constants, as discussed below. (See Refs. 14–16 for a further discussion.)

The biaxial Young's modulus of the grain boundary (the Young's modulus perpendicular to the boundary) was calculated by applying a small tensile stress (0.05% of the Young's modulus) to the crystal in the direction normal to the boundary. The atomic positions and dynamic boundaries were then adjusted to minimize the total energy of the system. In Fig. 4 we plot the resulting average Young's modulus of each layer parallel to the boundary, defined halfway between each (100) plane of atoms:

$$E^i=\frac{\sigma_{11}}{\epsilon_{11}^i}\ , \tag{2}$$

where σ_{11} is the applied stress, and the strain of each layer i is given by

$$\epsilon_{11}^i=\frac{\Delta x^i-\Delta x_0^i}{\Delta x_0^i}\ , \tag{3}$$

where Δx_0^i and Δx^i are the average interlayer spacings before and after applying the stress, respectively.

Between the free surface and the boundary, E^i is very close to the perfect crystal value (0.67 and 0.61×10^{12} erg/cm^3, respectively). The value for the slab is slightly higher than that for the bulk because the interplanar spacing is 1.822 Å instead of the bulk value of 1.807 Å; as shown in Fig. 1, this strain of 0.8% results in a 10% increase in the Young's modulus of the slab.

At the free surface, E^i is slightly higher than that for a perfect crystal. At the grain boundary, E^i is much higher than the perfect crystal value. Oscillations in the

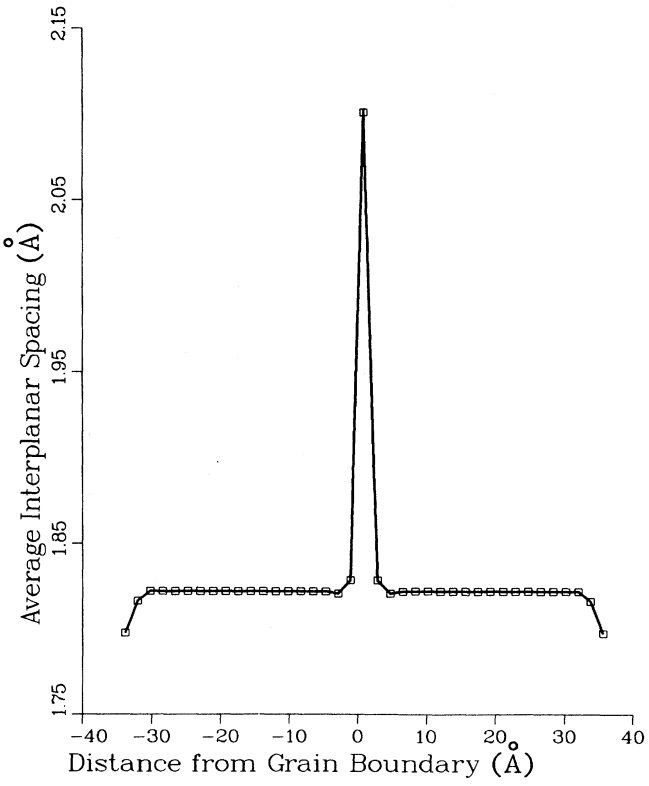

FIG. 3. Interplanar spacing as a function of distance across a slab containing a Σ5 twist grain boundary in its center. The slab has free surfaces at its minimum and maximum x coordinates.

modulus closely correspond to oscillations in the interplanar spacing (see Figs. 3 and 4).

The shear modulus for shears in the plane of the boundary was also calculated by applying a small shear stress (0.1% of the bulk shear modulus) to the crystal in the plane parallel to the boundary. The direction of the shear is the [100] direction of the reference lattice (each half of the crystal was rotated 18.4° relative to the reference lattice to create the $\Sigma 5$ twist boundary).

In Fig. 5 we plot the average shear modulus of each layer parallel to the boundary, defined halfway between each (100) plane of atoms:

$$C_{44}^{i}=\frac{\sigma_{12}}{\epsilon_{12}^{i}} \tag{4}$$

where the average strain of each layer is given by

$$\epsilon_{12}^{i}=\frac{dy^{i}}{\Delta x_{0}^{i}} \ . \tag{5}$$

dy^{i} is the difference in the average atomic displacement (in the direction of the shear) on either side of the layer.

Between the free surface and the boundary, C_{44}^{i} is very close to the perfect crystal value (0.75 and 0.76×10^{12} ergs/cm^3, respectively). At the free surface, C_{44}^{i} is slightly higher than that for a perfect crystal. At the grain boundary, C_{44}^{i} is approximately $\frac{1}{20}$ of the perfect crystal value. Oscillations in the modulus closely correspond to oscillations in the interplanar spacing (see Fig. 3).

Comparing Figs. 3–5 shows that the interplanar spacing appears to be closely correlated with the elastic properties, in that small deviations in the interplanar spacing correspond with large deviations of the layer elastic properties.

The interplanar spacing at the grain boundary is greater than for a perfect crystal, namely 15% at the first layer and 1% at the second. Thus, the atoms on either side of the boundary see an average 8% expansion. For a perfect crystal subject to a uniaxial strain of 8%, Figs. 1 and 2 show that E is increased by approximately 66% and C_{44} is decreased by 33%; this agrees qualitatively with the values of E_i (53% increase) and C_{44}^{i} (97% decrease) at the first layer on either side of the grain boundary. Since the elastic constants of the grain boundary are less than those of a similarly expanded crystal, it appears that the nonideal crystal structure at the boundary tends to lower the elastic moduli, especially C_{44}^{i}.

In summary, it appears that the elastic properties of the twist boundary are largely determined by the expansion of the boundary, and the structure of the boundary.

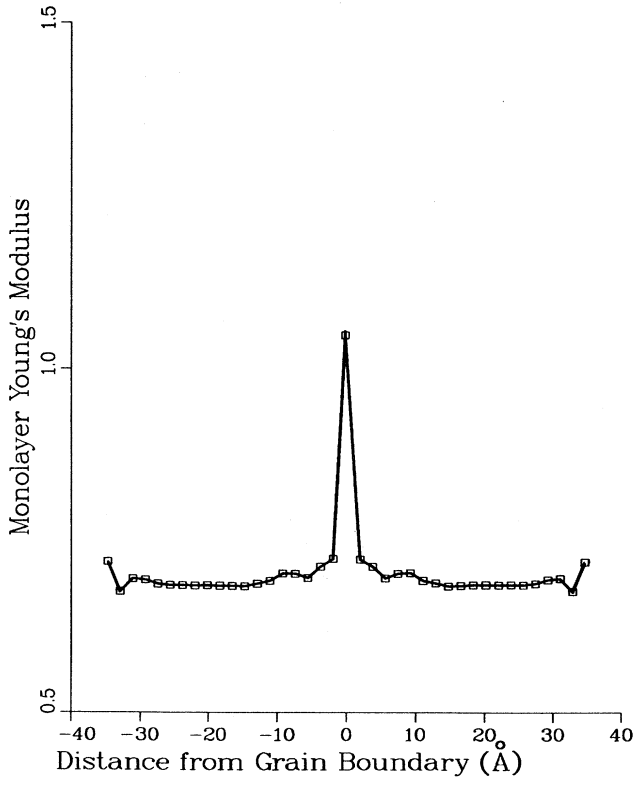

FIG. 4. The layer biaxial Young's modulus (in 10^{12} ergs/cm^3) for biaxial stresses acting on a $\Sigma 5$ twist grain boundary [see Eq. (2)].

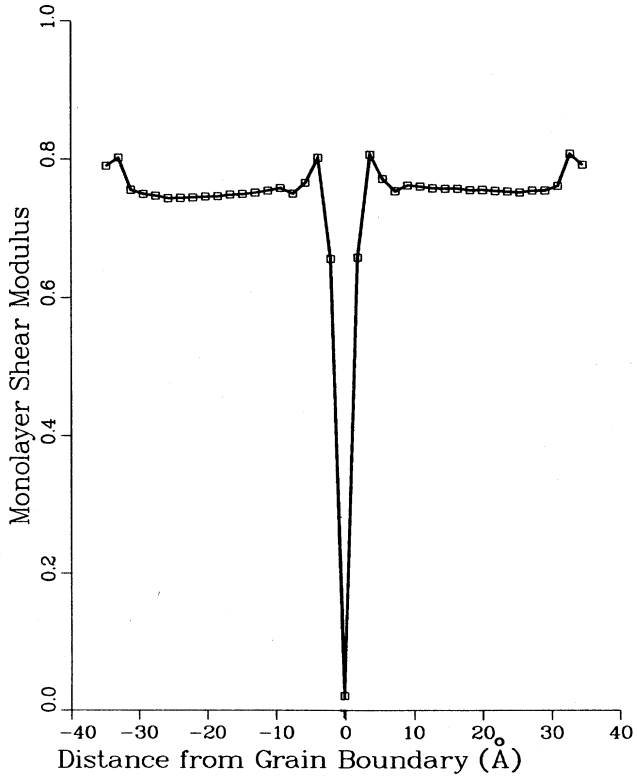

FIG. 5. The layer shear modulus (in 10^{12} ergs/cm^3) for a slab containing a $\Sigma 5$ twist grain boundary, subject to a shear parallel to the grain boundary [see Eq. (4)].

IV. SUMMARY

In this paper we have shown the following:

(1) The pressure derivatives of K, G, and C_{44} of copper were calculated and found to be in close agreement with experiment.

(2) The uniaxial strain derivative of the effective Young's modulus was calculated and found to be in close agreement with experiment.

(3) The uniaxial strain derivative of the shear modulus C_{44} (for no Poisson contraction) was calculated and found to be negative.

(4) The biaxial Young's and shear moduli of a $\Sigma 5$ twist grain boundary were calculated. They agreed qualitatively with the studies of grain boundary superlattices by Wolf and Lutsko,[14,15] who found an increase in the Young's modulus and a decrease in the shear modulus. This behavior is similar to that of a perfect crystal which has been expanded in one dimension.

(5) The nonideal crystal structure at the grain boundaries appears to weaken both the Young's moduli and especially the shear moduli of the $\Sigma 5$ twist grain boundary.

Further calculations on many different grain boundaries are required to determine if statements (4) and (5) are applicable to other types of boundaries than the one we studied. Since the uniaxial strain derivative of the Young's modulus has the opposite sign in the [110] and [111] directions than in the [100] direction, it is expected that the Young's moduli of twist boundaries with (110) and (111) faces will be *smaller* than the bulk value.

ACKNOWLEDGMENTS

We wish to thank Dr. Dieter Wolf of Argonne National Laboratories for his useful comments and suggestions, as well as for sharing his unpublished work with us. We also thank Dr. Mike Baskes and Dr. Murray Daw of Sandia National Laboratories, Livermore, California for their useful comments and suggestions. Work was supported by the U.S. Department of Energy, Office of Basic Energy Sciences, Division of Materials Science.

[1]T. Schober and R. W. Baluffi, Philos. Mag. **20**, 511 (1969).
[2]T. Schober and R. W. Baluffi, Philos. Mag. **21**, 108 (1970).
[3]W. Krakow and D. A. Smith, J. Mater. Res. **1**, 47 (1986).
[4]J. Budai, P. D. Bristowe, and S. L. Sass, Acta Metall. **31**, 698 (1983).
[5]M. R. Fitzsimmons and S. L. Sass, Acta Metall. (to be published).
[6]M. R. Fitzsimmons and S. L. Sass, Acta Metall. (to be published).
[7]I. Majid, P. D. Bristowe, and R. W. Baluffi, Phys. Rev. B **40**, 2779 (1989).
[8]P. D. Bristowe and A. G. Crocker, Philos. Mag. A **38**, 487 (1978).
[9]G.-J. Wang, A. P. Sutton, and V. Vitek, Acta Metall. **32**, 1093 (1984).
[10]P. D. Bristowe and R. W. Baluffi, J. Phys. (Paris) Colloq. **46**, C4-155 (1985).
[11]Y. Oh and V. Vitek, Acta Metall. **34**, 1941 (1986).
[12]S. M. Foiles, Acta Metall. (to be published).
[13]S. M. Foiles, M. I. Baskes, and M. S. Daw, in *Interfacial Structure, Properties, and Design,* edited by M. A. Yoo, W. A. T. Clark, and C. L. Briant (MRS, Pittsburgh, 1988).
[14]D. Wolf and J. F. Lutsko, Phys. Rev. Lett. **60**, 1170 (1988); (unpublished).
[15]D. Wolf, J. Lutsko, and M. Kluge, in *Proceedings of the Symposium on "Atomistic Modelling in Materials—Beyond Pair Potentials," Chicago, September, 1988* (Plenum, New York, in press).
[16]S. R. Phillpot, J. F. Lutsko, and D. Wolf (unpublished).
[17]M. S. Daw and M. I. Baskes, Phys. Rev. B **29**, 6443 (1984).
[18]S. M. Foiles, M. I. Baskes, and M. S. Daw, Phys. Rev. B **33**, 7983 (1986).
[19]S. M. Foiles and M. S. Daw, Phys. Rev. B **38**, 12 643 (1988).
[20]S. M. Foiles and J. B. Adams, Phys. Rev. B (to be published).
[21]W. G. Wolfer and J. B. Adams (unpublished).
[22]M. S. Daw and R. D. Hatcher, Solid State Commun. **56**, 697 (1985).
[23]S. M. Foiles, Phys. Rev. B **32**, 3409 (1985).
[24]J. B. Adams, S. M. Foiles, and W. G. Wolfer, J. Mater. Res. Dev. **4**, 102 (1989).
[25]J. B. Adams and W. G. Wolfer, J. Nucl. Mat. **158**, 25 (1988).
[26]M. S. Daw and S. M. Foiles, J. Vac. Sci. Technol. A **4**, 1412 (1986).
[27]M. S. Daw, Surf. Sci. **166**, L161 (1986).
[28]S. M. Foiles, Surf. Sci. **191**, L779 (1987).
[29]M. S. Daw and S. M. Foiles, Phys. Rev. Lett. **59**, 2756 (1987).
[30]S. M. Foiles, Phys. Rev. B **32**, 7685 (1985).
[31]S. M. Foiles, J. Vac. Sci. Technol. A **5**, 889 (1987).
[32]J. S. Nelson, E. C. Sowa, and M. S. Daw, Phys. Rev. Lett. **61**, 1977 (1988).
[33]J. S. Nelson, M. S. Daw, and E. C. Sowa, Phys. Rev. B **40**, 1465 (1989).
[34]J. F. Lutsko (unpublished).
[35]M. Parinello and A. Rahman, J. Appl. Phys. **52**, 7182 (1981).
[36]W. B. Daniels and C. S. Smith, Phys. Rev. **111**, 713 (1958).
[37]Y. Hiki and A. V. Granato, Phys. Rev. **144**, 411 (1966).
[38]K. Salama (private communication), reported by M. W. Riley and M. J. Skove, Phys. Rev. B **8**, 466 (1973).
[39]F. Milstein and D. Rasky, Philos. Mag. A **45**, 49 (1982).
[40]H. Kobayashi and Y. Hiki, Phys. Rev. B **7**, 594 (1973).
[41]M. W. Riley and M. J. Skove, Phys. Rev. B **8**, 466 (1973).